RESEARCH ARTICLE
Bull Biotechnol (2025) 6(1):1-10
https://doi.org/10.51539/biotech.1564289 Journal homepage: www.dergipark.org.tr/biotech

Bulletin of Biotechnology

Application of chitosan-alginate biocomposite for adsorption of Erythrosine B dye from wastewater: isotherm and kinetic study

Zeynep Mine Şenol[1*], Zehra Seba Keskin[2]

[*1]*Department of Nutrition and Diet, Faculty of Health Sciences, Sivas Cumhuriyet University, Sivas, Türkiye*
[2]*Department of Pharmacy, Health Services Vocational School, Sivas Cumhuriyet University, Sivas, Türkiye*

*Corresponding author: msenol@cumhuriyet.edu.tr
Orcid No: https://orcid.org/0000-0002-5250-126

Received : 10/10/2024
Accepted : 03/02/2025

To Cite: Şenol ZM, Keskin ZS (2025) Application of chitosan-alginate biocomposite for adsorption of Erythrosine B dye from wastewater: isotherm and kinetic study. Bull Biotechnol 6(1):1-10 https://doi.org/10.51539/biotech.1564289

Abstract: Biocomposite materials are effective and efficient adsorbents in the treatment of dye-contaminated wastewater. In this study, the adsorption properties of chitosan (Ch)-alginate (A) biocomposite for Erythrosine B (EB) dye were investigated. FT-IR, SEM-EDX, and zero-charge point analyses support the idea that the adsorption process may occur via hydrogen bonds and electrostatic interactions between dye molecules and functional groups on the surface of Ch-A biocomposite. The maximum adsorption capacity of Ch-A biocomposite was found to be 319 mg g^{-1}. The adsorption energy value was found to be 7.76 kJ mol^{-1}, which indicates the physical nature of the adsorption process. Adsorption kinetics showed that the adsorption process first occurs as rapid adsorption onto the surface and then as relatively slow intraparticle diffusion. Adsorption thermodynamic studies showed that the adsorption process is endothermic and spontaneous. When all adsorption studies are evaluated together, Ch-A biocomposite is an alternative, effective, efficient, and promising adsorbent for better environmental protection and public health safety in removing EB dye from wastewater. We hope this study can successfully guide the development of new and more powerful approaches to reduce EB dye pollution in wastewater. It is of critical importance to protect the environment and human health from the toxic effects of EB dye that threatens life and enters wastewater. Because a clean environment means a more livable world for future generations.

Keywords: Chitosan; alginate; biocomposite; Erythrosine B; removal; wastewater treatment

1 Introduction

Although water is one of the most abundant natural resources on earth, only about 0.007% is available for human consumption. As a result, billions of people today lack access to clean, drinkable water, and the demand is growing daily (Sağlam, Türk, and Arslanoğlu 2023) (Alsawat 2024). Furthermore, the discharge of wastewater, generated by rapid industrialization and urbanization, into natural water sources without treatment represents a significant challenge in terms of water access. The dyes present in this wastewater, due to their toxic and stable nature, cause visual and chemical pollution, thereby posing a considerable threat to the environment (M. F. Ahmad et al. 2024). The presence of dyes in wastewater impairs the photosynthetic activities of aquatic organisms and alters their biological processes. Furthermore, these dyes can undergo degradation into mutagenic, toxic, and carcinogenic compounds that pose a threat to the health of living organisms (Raji et al. 2023).

Erythrosine B is a member of the anionic xanthene dye class and exhibits high solubility in water. It is employed extensively in the food, cosmetic, and pharmaceutical industries (Nascimento et al. 2022). The World Health Organization (WHO) has established a maximum daily intake of EB at 0–1.25 mg kg^{-1} (Lai, Li, and Zhang 2021). However, ingestion of quantities over these limits can result in the development of allergic reactions, as well as carcinogenic and mutagenic effects, and thyroid disorders in humans (Pipíška et al. 2022). Given the detrimental impact of EB dye on public health and the natural environment, it is imperative to develop effective strategies for the treatment of wastewater contaminated with this substance. Consequently, a variety of techniques, including ion exchange, coagulation, membrane technology, chemical oxidation, photocatalytic degradation, ozonation, and adsorption, are utilized to eliminate synthetic dyes such as EB from wastewater (Umesh, Puttaiahgowda, and Thottathil 2024) (T. Ahmad et al. 2024).

Nevertheless, a disadvantage of these methods is the utilization of chemical reagents that result in secondary pollution and their considerable electricity costs. In contrast, adsorption is a more frequently preferred method due to its low cost, simplicity, environmental friendliness, process flexibility, and high efficiency (Umesh et al. 2024) (Arni et al. 2023). In the removal of dyes from aqueous solutions through adsorption, a variety of adsorbents have been employed, including activated carbon (Raji et al. 2023), biomass (Şenol, Messaoudi, et al. 2023), biochar (Zhang, He, and Liu 2023), graphene (Khan Rind et al. 2023), clays (Ighnih et al. 2023), nanocomposites (Rehan et al. 2023), and natural polymers (Hevira, Ighalo, and Sondari 2024). However, due to the high cost and toxicity of activated carbon, graphene, and carbon nanotubes, recent studies have focused on the effectiveness of natural polymers like chitosan and alginate, as well as biocomposites synthesized from them, in dye removal (Şen and Şenol 2023a).

Chitosan is a polysaccharide derived from the deacetylation of chitin and represents one of the most prevalent natural polymers on Earth. Chitosan is employed in a multitude of industries, including agriculture, medicine, biomedicine, food, paper, textiles, and cosmetics. The aforementioned characteristics of chitosan, namely its hydrophilicity, abundant availability, high biocompatibility, strong chemical reactivity, non-toxicity, low cost, recyclability, antimicrobial activity, and functional groups (-NH_2 and -OH) that support adsorption, render it an attractive adsorbent. Nevertheless, the utilization of chitosan (as an adsorbent is constrained by several factors, including its inadequate mechanical strength, limited specific surface area, susceptibility to depolymerization in acidic conditions, proclivity to agglomerate, and elevated swelling index (Abdulhameed et al. 2024) (Kashi et al. 2024) (Sabbagh, Tahvildari, and Mehrdad Sharif 2021). To enhance these structural characteristics, chitosan has been modified through techniques such as cross-linking, covalent grafting, and ionic liquid impregnation with minerals, metal nanoparticles, synthetic polymers, metal oxides, glutaraldehyde, clay, and polysaccharides like alginate (Issahaku, Tetteh, and Tetteh 2023). The utilization of cross-linkers, such as epichlorohydrin and tripolyphosphate, has the potential to enhance the surface properties, chemical stability, and mechanical strength of the synthesized biocomposite (Bellaj et al. 2024) (Hisham et al. 2024). Due to its abundant natural availability, low cost, non-toxicity, hydrophilic nature, biodegradability, and ability to cross-link with divalent cations, various studies have reported that chitosan can be cross-linked to synthesize a biocomposite with enhanced properties (Şenol, Elma, et al. 2023). Additionally, in several studies, chitosan's high amino functional groups have been shown to attract dye anions through electrostatic interactions (Chiou and Chuang 2006) (Chiou, Ho, and Li 2004).

Alginate, a linear polysaccharide derived from brown seaweed, is a widely utilized material in a multitude of industries, including cosmetics, pharmaceuticals, textiles, food production, and the manufacture of medical products (Kazemi and Javanbakht 2020). The alginate is a natural anionic biopolymer with free hydroxyl (–OH) and carboxyl (–COOH) groups. It has attracted great attention due to its widespread availability, low cost, biocompatibility, and biodegradability. Its ability to bind metal cations (usually divalent cations) through ionic interactions has made alginate an alternative to traditional treatment methods for heavy metal removal. However, the poor mechanical and chemical resistance of this biopolymer limits its industrial use on a large scale (Sachan 2009). One of the new approaches used to solve this disadvantage of biopolymers is to use them as composite material components.

This paper investigated the adsorption properties of Ch-A biocomposite cross-linked with tripolyphosphate and epichlorohydrin to effectively remove anionic EB dye from aqueous solutions. Extensive research in the literature revealed that this study is the first to investigate the performance of cross-linked Ch-A biocomposite in the removal of EB dye. The effects of initial EB concentration, pH, contact time, adsorbent dose, and temperature on the adsorption process were investigated. Furthermore, the adsorption mechanism was explained using isotherm and kinetic models and the adsorption capacity for EB dye was evaluated. The findings demonstrated that Ch-A biocomposite is an effective, environmentally friendly, and cost-effective alternative adsorbent for the removal of EB dye.

2 Materials and Method

2.1 Chemicals

The EB ($C_{20}H_6I_4Na_2O_5$) dye was purchased from Merck (Germany). The chemical structure of EB was given in Fig. 1. Medium molecular weight Ch, A, epichlorohydrin (ECH), NaOH, sodium tripolyphosphate (NaTPP), KNO_3, and HCl, were obtained from Sigma-Aldrich.

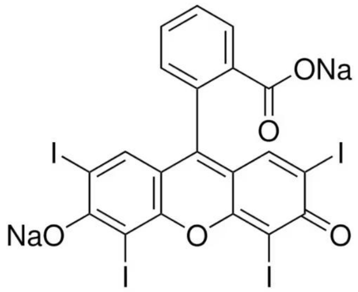

Fig. 1 Chemical structure of EB

2.2 Preparation of Ch-A biocomposite beads

In the synthesis of Ch-A biocomposite beads, the method of (Şenol 2021) was followed. Then, the Ch-A biocomposite was ground into powder and stored.

2.3 Batch adsorption experiments

The batch experimental conditions are given in Table 1. The EB dye concentration was determined at 528 nm (Kaur and Datta 2013) in a UV–vis spectrophotometer. Removal% and

Q adsorbed amount of EB dye (mg g^{-1}) were calculated using Eq. 1 and Eq. 2.

$$Removal\% = \left[\frac{C_i - C_f}{C_i}\right] x100 \qquad \textbf{(1)}$$

$$Q = \left[\frac{C_i - C_f}{m}\right] xV \qquad \textbf{(2)}$$

Table 1. Experimental conditions

Aim of experiment	**pH**	**[EB]$_0$ (mg L^{-1})**	**m (g L^{-1})**	**t (min)**	**T (^{0}C)**
Effect of pH	2.0-12.0	500	5	1440	25
Effect of concentration	6.5	10-1000	5	1440	25
Effect of time	6.5	500	15	2-1440	25
Effect of adsorbent dose	6.5	500	1, 3, 5, 10	1440	25
Effect of temperature	6.5	500	5	1440	5, 25, 40

3 Results

3.1 FT-IR and SEM-EDX analysis

The FT-IR spectra of Ch, A, and the Ch-A biocomposite are shown in Fig. 2. The broad band observed in the FTIR spectrum of chitosan (Ch) between 3656 and 3010 cm^{-1} is attributed to the stretching vibrations of N-H and O-H. The peaks observed at 2882, 1619, and 1538 cm^{-1} are attributed to the stretching of the C-H bond, the bending of the N-H bond, and the bending of the primary amine N-H bond, respectively (He et al. 2023) (Benhouria et al. 2023). The distinctive peaks of chitosan at 1438, 1329, and 1032 cm^{-1} are attributed to C-O stretching, and C-H bending, (Tran et al. 2023) (Meng et al. 2023) (Şenol and Şimşek 2020). The broad band observed in the FT-IR spectrum of alginate between 3676 and 2975 cm^{-1} is attributed to O-H group stretching vibrations. The peak at 2914 cm^{-1} is attributed to C-H stretching, while the peaks at 1599 and 1407 cm^{-1} are assigned to COO$^-$ group stretching vibrations. The peak at 1081 cm-1 is associated with C-H bending, and the peak at 1028 cm^{-1} corresponds to C-O stretching vibrations (Nandanwar et al. 2023) (Wen et al. 2024) (Khapre, Pandey, and Jugade 2021). The FT-IR spectrum of the Ch-A biobiocomposite displays the presence of characteristic peaks at 2882, 1619, and 1538 cm^{-1}, which are associated with chitosan, and peaks at 1407, 1081, and 1028 cm^{-1}, which are characteristic of alginate. The appearance of these peaks serves as confirmation that the synthesis of the biocomposite was accomplished.

The FT-IR spectra of the Ch-A biocomposite are presented in Fig. 2, illustrating the spectra of the biocomposite before adsorption and after the adsorption of the EB dye. A comparison of the FT-IR spectra of the EB-loaded Ch-A biocomposite with that of the unloaded Ch-A spectrum reveals notable differences. Following the adsorption of EB dye molecules, alterations in the position and intensity of the characteristic peaks of Ch-A can be ascribed to the electrostatic interaction between the EB dye molecules and Ch-A bio. Furthermore, the emergence of new peaks in the FT-IR spectrum of EB-loaded Ch-A at 645 cm^{-1} and 1326 cm^{-1} can be attributed to the C-I stretching vibration of the EB dye (Ramalakshmi, Murugan, and Jeyabal 2022) and the C-H deformation of the xanthene ring (Kaur and Datta 2013), respectively. The broadband for O-H and N-H seen around 3200-3500 cm^{-1} has shifted and increased in intensity due to the hydrogen bonding of EB and biocomposite. It was observed that the intensities of amide I and amide II bands increased around 1650 cm^{-1} and 1560 cm^{-1}, which indicates the interaction of the biocomposite with EB dye. The increases in the intensity of the peaks seen around 1600 cm^{-1} and 1400 cm^{-1} corresponding to the carboxylate groups indicate the interaction of the carboxylate groups of alginate with EB dye and were evaluated as evidence for EB dye adsorption.

The structures constituting the Ch-A biocomposite and its components and the SEM images and EDX spectra after EB adsorption are presented comparatively in Fig. 3(a-d). The SEM images revealed that chitosan possesses a porous surface (Fig. 3(a)), whereas alginate exhibits a rough and porous structure (Fig. 3(b)). The SEM image of the Ch-A biocomposite (Fig. 3(c)) has a completely different morphology from its components. After EB adsorption, there is a significant change in the surface morphology of the Ch-A biocomposite and its surface appears to have become smoother (Fig. 3(d)). This may be due to surface complexation. EDX spectra showed that Ch contained C, N, and O (Fig. 3(e)), while alginate contained C, O, and Na (Fig. 3(f)). The Ch-A biocomposite showed that both Ch and alginate contained C, N, O, and Na elements (Fig. 3(g)). The EDX data of the Ch-A biocomposite after EB adsorption (Fig. 3(h)) confirms the adsorption of the dye, as does the presence of iodine, which is not present in the elemental composition of Ch-A.

3.2 Effect of pH of EB dye solution

Adsorption efficiency is strongly dependent on the pH of the solution medium. The pH of the solution medium is affected by the surface properties of the adsorbent and the ionization of the dye molecules. The pH effect on the adsorption of EB dye molecules onto the Ch-A composite was investigated in the pH range of 2.0-12.0 (Fig. 4). EB is an acidic dye and since the functional groups of acidic dyes are anionic, they release negative charges to their aqueous solutions. Acid dyes have chromophore groups with negative electrical charges. At acidic pH values, the adsorbent surface is positive due to the high concentration of H$^+$ ions. This increases the electrostatic interaction between the adsorbent and the anionic dye molecules. In acidic conditions, the electrostatic interactions between the positively charged adsorbent surface and the COO$^-$ groups of the EB dye molecules play an important role in the adsorption process. Therefore, the adsorption efficiency was found to be high at pH: 2.0. In the pH range of 4.0-12.0, it was observed that the adsorption efficiency gradually decreased. With increasing pH values, the number of negatively charged sites on the adsorbent surface increases and the number of positively charged sites decreases. The lower adsorption efficiency under alkaline conditions is due to the competition between anionic EB dye molecules and OH- ions for adsorption sites. The surface of the adsorbent was negatively charged at basic pH values, which hindered the adsorption of anionic EB dye molecules by electrostatic repulsion (Pan and Zhang 2009). In addition to the electrostatic interactions between the Ch-A composite adsorbent and anionic EB dye molecules, intermolecular interactions such as physical forces such as hydrogen bonding also occur (Ansari and Mosayebzadeh 2010). The surface charge of the adsorbent was found by point of zero charge (pHpzc) analysis (Şenol et al. 2024). The surface charge of the Ch-A composite adsorbent was found to be 4.59 (Fig. 4). The Ch-A composite will be positively charged in solutions with pH below the pHpzc value and negatively charged in solutions with pH above it. At strong acidic pH values (pH<pHpzc), the adsorbent surface will be positively charged and the anionic EB dye adsorption efficiency will increase. At basic pH values (pH>pHpzc), hydroxyl ions deprotonate all nitrogen atoms in the Ch-A composite adsorbent and the surface charge becomes significantly negative. In this case, the adsorption efficiency also decreased. These two sets of findings were in agreement with the predicted framework for the pH effect on the removal of EB dye molecules onto the Ch-A biocomposite.

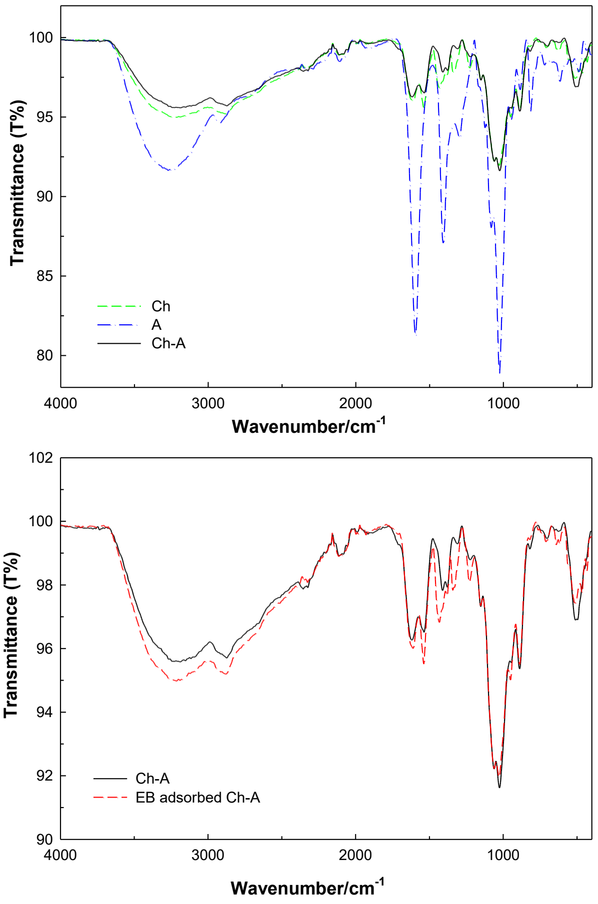

Fig. 2 FT-IR spectrum of Ch, A, Ch-A, and EB adsorbed Ch-A biocomposite

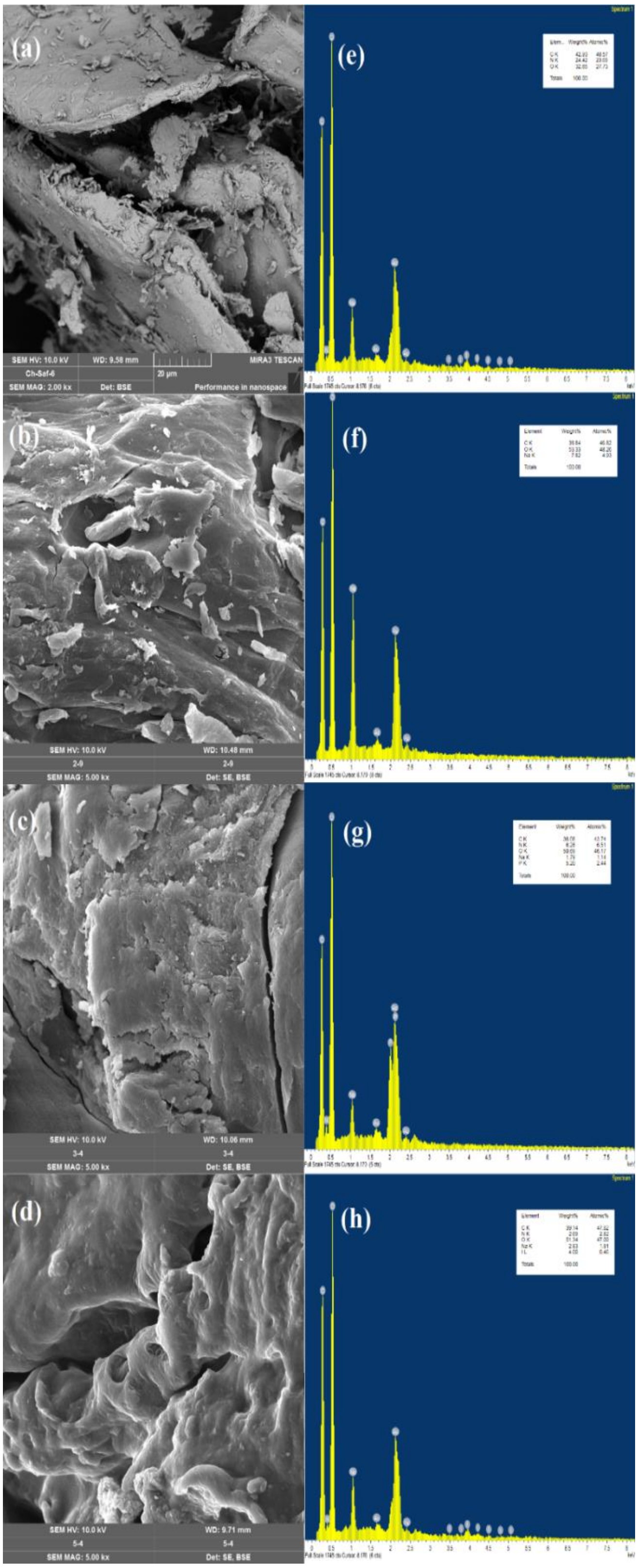

Fig. 3 SEM morphologies of Ch (a), A (b), Ch-A (c), and EB adsorbed Ch-A (d) and EDX spectra of Ch (e), A (f), Ch-A (g), and EB adsorbed Ch-A (h)

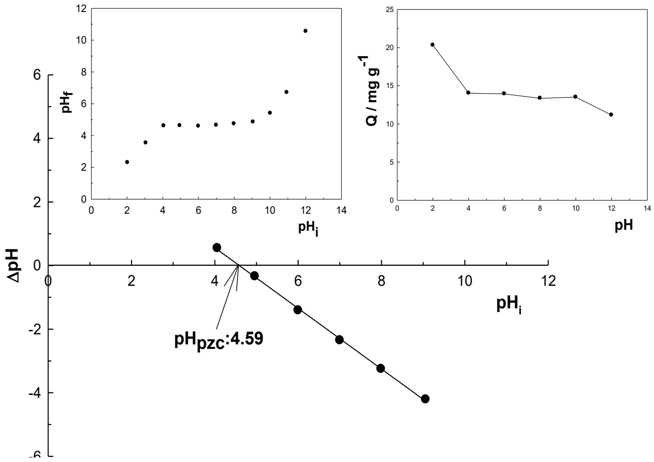

Fig. 4 Effect of pH and pHpzc for Ch-A

3.3 Effect of the biocomposite dose

The efficiency of dye removal from wastewater is contingent upon the number of active adsorption sites on the adsorbent surface. The determination of the optimal quantity of adsorbent to be employed represents a pivotal element in the evaluation of the cost per unit of dye solution (Elgarahy et al. 2021). The impact of varying concentrations of Ch-A (1-20 g L^{-1}) on the adsorption of EB dye molecules was examined while maintaining other experimental variables at a constant level. Fig. 5 illustrates the relationship between the percentage removal of EB dye and the adsorption capacity of Ch-A concerning the adsorbent amount. The increase in the amount of Ch-A resulted in a notable enhancement in the percentage removal of EB dye, rising from 88% to 94% (Fig. 5). This increase can be attributed to the proportional rise in the number of active binding sites and surface area with the greater amount of Ch-A. Consequently, anionic EB dye molecules are more readily retained by the active centers on the Ch-A surface (Şen and Şenol 2023b). Nevertheless, the augmented Ch-A quantity resulted in a reduction in the quantity of EB dye adsorbed per unit. This reduction can be attributed to the fact that the increased number of active sites on Ch-A may not have reached saturation with the EB dye molecules, resulting in the clustering of adsorption sites and longer diffusion distances. The highest adsorption capacity identified was achieved with a 1 g L^{-1} adsorbent dose (Ezeh et al. 2017).

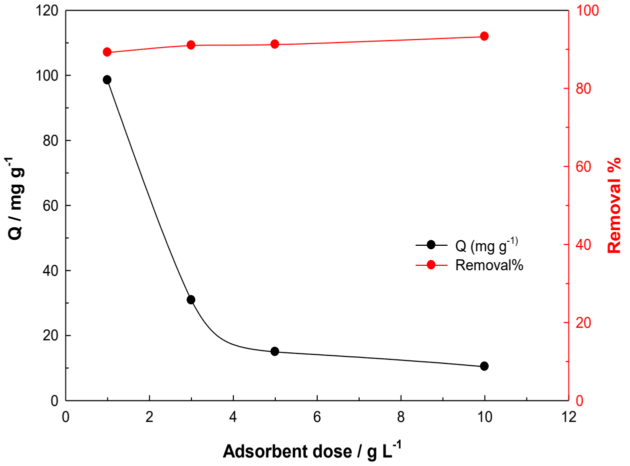

Fig. 5 Effect of the biocomposite dose

3.4 Modeling of Adsorption Process

In this study, Langmuir (Langmuir 1918), Freundlich (Freundlich 1907), and Dubinin-Radushkevich (D-R) (Dada 2012) isotherm models, were applied to the experimental data. The adsorption behavior of EB dye on Ch-A composite was analyzed using isotherm models and the fit of the isotherm plots is presented in Fig. 6. The derived isotherm parameters are listed in Table 2. Fig. 6 shows that the adsorption efficiency of EB dye is high at low concentrations due to the presence of vacant active sites on the surface of the Ch-A biocomposite. However, at higher concentrations, these active sites are filled and the adsorption efficiency decreases and eventually, equilibrium is reached. When the R^2 values from the Langmuir and Freundlich isotherm models are compared (Fig. 6, Table 2), it is seen that the adsorption is in good agreement with the Langmuir isotherm model. The maximum adsorption capacity obtained from this model is 319 mg g^{-1} and the Langmuir constant is 0.00227 L mg^{-1}. The high adsorption capacity of the Ch-A biocomposite indicates its potential as an effective adsorbent for removing EB dye from wastewater. According to the Freundlich isotherm model, the adsorption capacity (X_F) was found to be 0.113 and the surface heterogeneity factor (β) was found to be 0.908. The adsorption energy calculated from the D-R model indicates that the adsorption process is physical. A comparison of the EB dye adsorption capacities of various adsorbents (Table 3) shows that the Ch-A composite exhibits a relatively high sorption capacity (319 mg g^{-1}).

Table 2. Isotherm parameters

Isotherm model	Parameter	Value
Langmuir	Q_L (mg g^{-1})	319
$Q = \frac{Q_L C_e}{1 + K_L C_e}$	K_L x10^3 (L mg^{-1})	2.27
	R^2	0.991
Freundlich	X_F	0.113
$Q = X_F C_e^{\beta}$	β	0.908
	R^2	0.989
D-R	X_{DR} (mg g^{-1})	774
$Q = X_{DR} e^{-(K_{DR}\varepsilon^2)}$	-K_{DR}x10^9/mol^2 KJ^{-2}	8.31
$\varepsilon = RT\ln\left(1 + \frac{1}{C_e}\right)$	E_{DR}/kJ mol^{-1}	7.76
$E_{DR} = (2K_{DR})^{-0.5}$	R^2	0.977

Table 3. Comparison of adsorption capacity for adsorption of EB dye on various adsorbents reported in the literature

Adsorbent	pH	Q/ mg g^{-1}	Reference
Montmorillonite	7.5	578.03	(Kaur and Datta 2013)
Pumpkin seed hulls	-	16.4	(Carmen Apostol et al. 2016)
Chitosan/ hydrogel SiO_2 hybrid material	-	71.27	(Copello et al. 2011)
Chitin/hydrogel SiO_2 hybrid material	-	131.98	(Copello et al. 2011)
Crystal violet modified montmorillonite	-	123.18	(Rytwo et al. 2006)
Bottom ash and de-oiled soya	2.0	16.17 and 9.52	(Mittal et al. 2006)
Sugarcane bagasse	9.0	500	(Sharma and Kaur 2011)
TiO_2 and ZnO surfaces	5.0-6.8	17.54 and 3.06	(Hasnat et al. 2007)
Cross-linked lysozyme crystals	-	70.39	(Cvetkovic et al. 2005)
Hen feathers	3.0	15.43	(Gupta et al. 2006)
Ch-A biocomposite	6.5	319	This study

3.5 Effect of contact time

In the adsorption process, it is vital that the adsorption reaches equilibrium in a short time. Kinetic studies help us predict the mechanism of the adsorption process at the solid-liquid interface. In the adsorption process, the solution transfer at the solid-liquid interface is expressed as either external mass transfer (boundary layer diffusion), intraparticle diffusion, or both. In general, three steps accompany the adsorption process; i) transport of the adsorbate from the bulk solution to the external surface of the adsorbent via the liquid film ii) diffusion of the adsorbate into the pores of the adsorbent iii) sorption of the adsorbate from the pores of the adsorbent to the inner surface of the capillary cavities. The third step is considered as an equilibrium reaction. The third of these three steps is assumed to be fast and negligible.

Upon examining the adsorption kinetics presented in Fig. 7, it is observed that the adsorption of EB dye increases with contact time. Adsorption efficiency increases rapidly until the first 300 minutes. After the 300 minutes, it is seen that the adsorption rate decreases and reaches equilibrium. The high adsorption rate observed in the first 300 minutes is due to the number of vacant active centers on the Ch-A composite surface. As a result, the interactions between the EB dye molecules in the solution and the active centers on the Ch-A composite surface have increased. Over time, the number of active centers has decreased due to the attachment of EB dye molecules to the vacant active centers on the Ch-A composite surface. This causes the adsorption rate to decrease after the 300 minutes. To study the effect of contact time on the adsorption process in detail, the kinetic data were analyzed as pseudo-first-order (PFO) (Ho and McKay 1998), pseudo-second-order (PSO) (Ho and McKay 1999) and intraparticle diffusion (IPD) (Wu, Tseng, and Juang 2009) the fit to the velocity models were investigated (Fig. 7).

The parameters obtained from the fit of PFO, PSO, and IPD kinetic models are summarized in Table 4. When the kinetic parameters in Table 4 are examined, it is seen that the adsorption process provides a better fit to the PSO kinetics. In addition, the experimental Q_t values and the theoretically calculated Q_e values are much closer to each other, which reveals the fit of the PSO model. In addition, the multicollinearity observed in the IPD plot indicates that the adsorption process involves two or more steps. Therefore, the adsorption of EB dye on the Ch-A composite can be described using both PSO and IPD models instead of a single kinetic model.

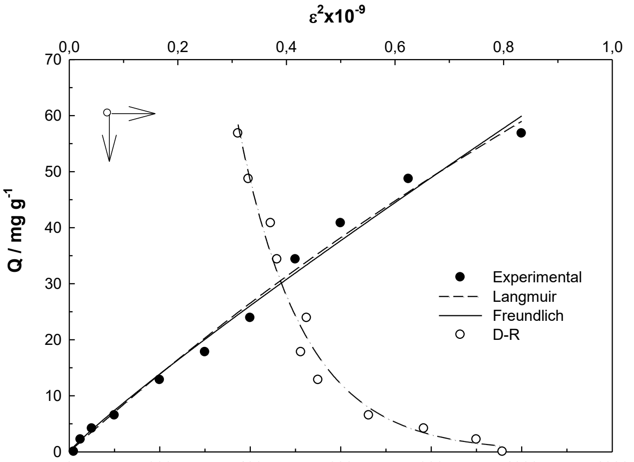

Fig. 6 Adsorption isotherms

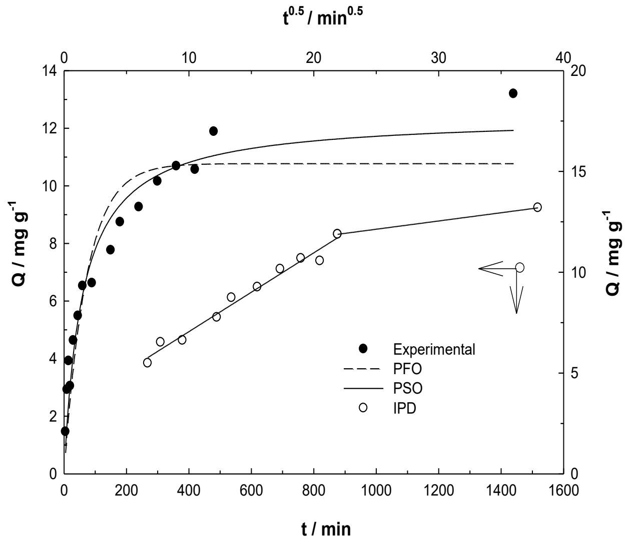

Fig. 7 Adsorption kinetics

Table 4. Kinetic parameters

Kinetic model	Parameter	Value
PFO	Q_t/mg g^{-1}	13.2
$Q_t = Q_e[1 - e^{-k_1 t}]$	Q_e/mg g^{-1}	10.8
$H_1 = k_1 Q_e$	k_1 x10^3/min^{-1}	13.9
	H_1x10^3/mg g^{-1} min^{-1}	150
	R^2	0.883
PSO	Q_t/mg g^{-1}	13.2
$Q_t = \frac{t}{\left[\frac{1}{k_2 Q_e^2}\right] + \left[\frac{t}{Q_e}\right]}$	Q_e/mg g^{-1}	12.4
	k_2 x10^3/mg^{-1} g min^{-1}	1.36
	H_2x10^3/mg g^{-1} min^{-1}	209
$H_2 = k_2 Q_e^2$	R^2	0.951
IPD	k_i x10^3/mg g^{-1} $min^{-0.5}$	3143
$Q_t = k_i t^{0.5}$	R^2	0.978

3.6 Effect of temperature

An investigation into the effect of temperature on adsorption allows insights to be gained into the thermodynamic parameters, which in turn facilitate an understanding of the process's feasibility and efficiency. To elucidate the nature of EB dye adsorption by Ch-A and its relationship with temperature, thermodynamic studies were conducted at 278, 298, and 313 K. The resulting data enabled the calculation of thermodynamic parameters, including enthalpy change (ΔH°), Gibbs free energy (ΔG°), and entropy change (ΔS°), using the following equations (Eq. 3-6) (Lima et al. 2019).

$$K_d = \frac{Q}{C_e} \qquad \textbf{(3)}$$

$$\Delta G^{\circ} = -RTln(K_d) \qquad \textbf{(4)}$$

$$lnK_D = \frac{\Delta S^{\circ}}{R} - \frac{\Delta H^{\circ}}{RT} \qquad \textbf{(5)}$$

$$\Delta G^o = \Delta H^o - T\Delta S^o \qquad \textbf{(6)}$$

Here, K_D represents the equilibrium adsorption rate constant (L mol^{-1}), R denotes the universal gas constant (8.314 J mol^{-1} K^{-1}), and T stands for the absolute temperature (K). The ΔH° and ΔS° parameters were calculated from the slope and the intercept of the line obtained from the lnK_D-1/T graph, which was drawn using the Van't Hoff equation, respectively (Fig. 8). The resulting values are presented in Table 5. The negative value of ΔH° (-15.4 kJ mol^{-1}) indicates that the adsorption of the EB dye onto Ch-A is exothermic and occurs physically. In general, ΔH° values in the range of -2.1 to -20.9 kJ mol^{-1} are indicative of physical adsorption, while values between -80 and -200 kJ mol^{-1} are indicative of chemical adsorption (Nannu Shankar et al. 2023). The positive ΔS° value (46.6 J mol^{-1} K^{-1}) indicates that during the adsorption of EB onto Ch-A, there is an increase in the degrees of freedom at the solid-liquid interface. This can also be attributed to the high affinity of Ch-A for the EB dye molecules. As demonstrated in Table 3, the negative ΔG° values at varying temperatures indicate that the adsorption process of the EB dye is both feasible and spontaneous, with favorable outcomes. Furthermore, the reduction in ΔG° values with rising temperature indicates that elevated temperatures serve as a driving force for adsorption (Akdemir et al. 2023). Furthermore, the observed increase in ΔG° values with rising temperature indicates that a greater driving force is required for adsorption at higher temperatures.

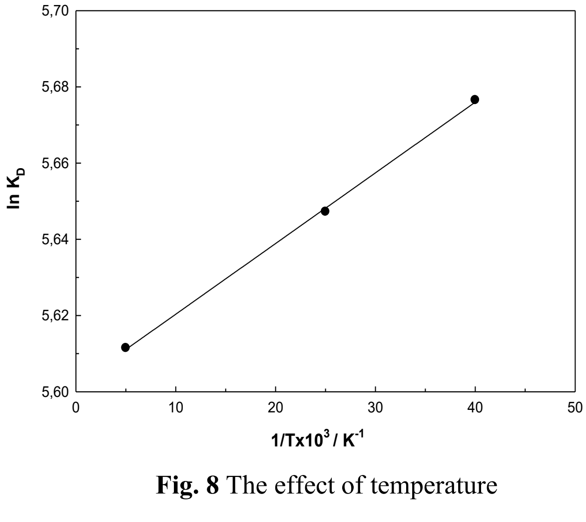

Fig. 8 The effect of temperature

Table 5. Thermodynamic parameters

T (°C)	ΔH⁰ (kJ mol^{-1})	ΔG⁰ (kJ mol^{-1})	ΔS⁰ (Jmol^{-1} K^{-1})	R^2
5		-28.4		
25	-15.4	-29.3	46.6	0.999
40		-30.1		

3.7 Possible removal mechanism

Fig. 9 shows the possible interactions between Ch-A biocomposite and EB dye molecules. The adsorption process of anionic EB dye molecules with Ch-A biocomposite is accompanied by multiple mechanisms such as H-bonding and electrostatic interactions. Amine groups on the surface of the Ch-A biocomposite can be easily protonated and anionic EB dye molecules can be bonded by electrostatic interaction. In addition, H-bonding can occur between electronegative groups of dye molecules and active centers on the surface of Ch-A biocomposite. In this study, electrostatic interactions and H-bonding were important factors in the entire adsorption process.

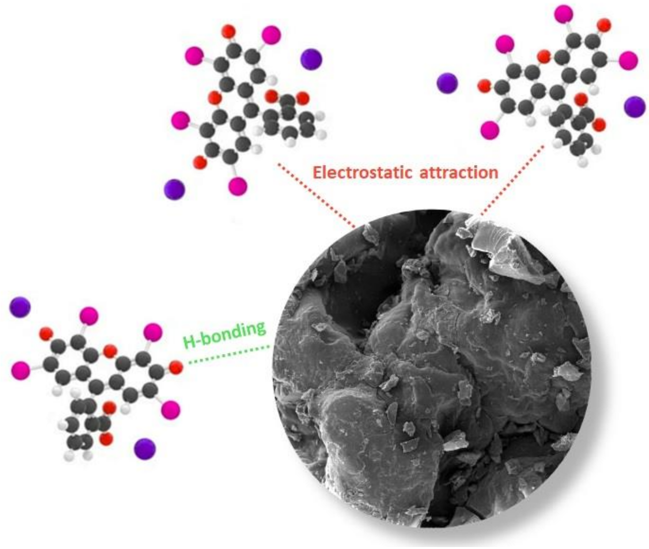

Fig. 9 Possible interactions of EB dye onto the Ch-A

5 Conclusion

In this study, the removal of EB dye from an aqueous solution was investigated using Ch-A biocomposite. Maximum adsorption capacity was achieved at pH 6.5 at 25 ºC. The maximum adsorption capacity of the Ch-A biocomposite for EB dye was found to be 319 mg g^{-1} at 25 °C (R^2 values, Langmuir isotherm model). Thus, the results fitted best the Langmuir model. The adsorption energy showed that adsorption was physical. Adsorption kinetics showed that the adsorption process followed the PSO and IPD patterns. Adsorption thermodynamics showed that the adsorption process is endothermic, entropy-increasing, and spontaneous. All obtained results showed that the Ch-A biocomposite will be an alternative, effective, and efficient adsorbent material for the removal of colored pollutants from wastewater.

Acknowledgements

This study was presented as an oral presentation at the 7th International Eurasian Conference on Biological and Chemical Sciences (EurasianBioChem 2024).

The present study was supported by the Sivas Cumhuriyet University Projects Commission (Project number: SBF-2023-101).

Authors' contributions:

ZMŞ: experimental work, visualization, supervision, writing, guidance, editing, and review

ZSK: writing, editing, and review

Conflict of interest disclosure:

The authors declare no conflict of interest.

References

Dada AO (2012) Langmuir, Freundlich, Temkin and Dubinin–Radushkevich Isotherms Studies of Equilibrium Sorption of Zn2+ Unto Phosphoric Acid Modified Rice Husk. IOSR J Appl Chem 3(1):38–45. doi: 10.9790/5736-0313845.

Abdulhameed AS, Mohammad KAK, Hassan A, Mohammad KY, and Sameer A (2024) Newly Developed Polymer Nanocomposite of Chitosan-Citrate/ZrO2 Nanoparticles for Safranin O Dye Adsorption: Physiochemical Properties and Response Surface Methodology. Mater Chem Phys 324:129699. doi: 10.1016/j.matchemphys.2024.129699.

Ahmad MF, Safia H, Zahid I, Danial M, Sumra A, Syed AU (2024) Green Approach to Water Purification: Investigating Methyl Orange Dye Adsorption Using Chitosan/Polyethylene Glycol Composite Membrane. J Polym Environ 32(1). doi: 10.1007/s10924-023-02994-9.

Ahmad T, Mohammad SM, Sardaraz K, Manal A. Al-Sharafi, Jordana G, Dison S.P.F, Nisar U (2024) Enhanced Adsorption of Bisphenol-A from Water through the Application of Isocyanurate Based Hyper Crosslinked Resin. J Mol Liq 395:123861. doi: 10.1016/j.molliq.2023.123861.

Akdemir M, Birol I, Fatih C, and Ozlem C (2023) High-Performing Natural Materials (Leonurus Cardiaca): Dye Biosorption Studies and Statistical Analysis. Biomass Convers Biorefin 13(15). doi: 10.1007/s13399-023-04469-2.

Alsawat M (2024) Congo Red Dye Adsorption Using CuSnO2TiO2 Nanocomposites: Adsorption Data Interpretation by Statistical Modeling. Int J Electrochem Sci 19(7):100611. doi: 10.1016/j.ijoes.2024.100611.

Ansari R, Zahra M (2010) Removal of Eosin Y, an Anionic DYE, from Aqueous Solutions Using Conducting Electroactive Polymers. Iran Polym J 19(7).

Arni LA, Ahmad H, Ahmed SA, Tumirah K, Zeid A, ALOthman LD, Wilson AHJ (202) Design of Separable Magnetic Chitosan Grafted-Benzaldehyde for Azo Dye Removal via a Response Surface Methodology: Characterization and Adsorption Mechanism. Int J Biol Macromol 242. doi: 10.1016/j.ijbiomac.2023.125086.

Bellaj M, Khalid A, Mounir EA, Mohammadine EH, Lhoucine G, Tonni AK, Zhonghao C, Pow SY, Faissal A (2024) Cationic and Anionic Dyes Adsorption from Wastewater by Clay-Chitosan Composite: An Integrated Experimental and Modeling Study. Chem Eng Sci 285. doi: 10.1016/j.ces.2023.119615.

Benhouria A, Zaghouane-Boudiaf H, Riadh B, Ferhat D, Hameed BH, Mokhtar B (2023) Cross-Linked Chitosan-Epichlorohydrin/Bentonite Composite for Reactive Orange 16 Dye Removal: Experimental Study and Molecular Dynamic Simulation. Int J Biol Macromol 242. doi: 10.1016/j.ijbiomac.2023.124786.

Carmen A, Laura, CG, Madalena A, Maria G (2016) Removal of Erythrosine B Dye from Water Effluents Using Crop Waste Pumpkin Seed Hulls as Adsorbent. Desalin Water Treat 57(47).

doi: 10.1080/19443994.2015.1132477.

Chiou MS, Guo SC (2006) Competitive Adsorption of Dye Metanil Yellow and RB15 in Acid Solutions on Chemically Cross-Linked Chitosan Beads. Chemosphere 62(5). doi: 10.1016/j.chemosphere.2005.04.068.

Chiou MS, Pang YH, Hsing YL (2004) Adsorption of Anionic Dyes in Acid Solutions Using Chemically Cross-Linked Chitosan Beads. Dyes and Pigm 60(1). doi: 10.1016/S0143-7208(03)00140-2.

Copello GJ, Andrea MM, Raineri M, Mariela PP, Luis ED (2011) Removal of Dyes from Water Using Chitosan Hydrogel/SiO2 and Chitin Hydrogel/SiO2 Hybrid Materials Obtained by the Sol-Gel Method. J Hazard Mater 186(1). doi: 10.1016/j.jhazmat.2010.11.097.

Cvetkovic A, Adrie JJS, Rajamani K, Luuk AMVDW (2005) Adsorption of Xanthene Dyes by Lysozyme Crystals. Langmuir 21(4). doi: 10.1021/la0478090.

Elgarahy AM, Elwakeel KZ, Mohammad SH, Elshoubaky GA (2021) A Critical Review of Biosorption of Dyes, Heavy Metals and Metalloids from Wastewater as an Efficient and Green Process. Clean Eng Technol 4:100209. doi: 10.1016/j.clet.2021.100209

Ezeh K, Ogbu IC, Akpomie KG, Ojukwu NC, Ibe JC (2017) Utilizing the Sorption Capacity of Local Nigerian Sawdust for Attenuation of Heavy Metals from Solution: Isotherm, Kinetic, and Thermodynamic Investigations. Pac J Sci Technol 18(1).

Freundlich H (1907) Über Die Adsorption in Lösungen. *Zeitschrift Für Physikalische Chemie* 57U(1). doi: 10.1515/zpch-1907-5723.

Gupta VK, Alok M, Lisha K, Jyoti M (2006) Adsorption of a Hazardous Dye, Erythrosine, over Hen Feathers. J Colloid Interface Sci 304(1). doi: 10.1016/j.jcis.2006.08.032.

Hasnat MA, Uddin MM, Samed AJF, Alam SS, Hossain S (2007) Adsorption and Photocatalytic Decolorization of a Synthetic Dye Erythrosine on Anatase TiO2 and ZnO Surfaces. J Hazard Mater 147(1–2). doi: 10.1016/j.jhazmat.2007.01.040.

He F, Baozhong M, Chengyan W, Yongqiang C, Xiujuan H (2023) Adsorption of Pb(II) and Cd(II) Hydrates via Inexpensive Limonitic Laterite: Adsorption Characteristics and Mechanisms. Sep Purif Technol 310:123234. doi: 10.1016/J.SEPPUR.2023.123234.

Hevira L, Joshua OI, Dewi S (2024) Chitosan-Based Polysaccharides for Effective Synthetic Dye Adsorption. J Mol Liq 393.

Hisham F, Maziati Akmal MH, Farah Ahmad KA, Noorasikin S (2024) Biopolymer Chitosan: Potential Sources, Extraction Methods, and Emerging Applications. Ain Shams Eng 15(2).

Ho YS, McKay G (1999) Pseudo-Second Order Model for Sorption Processes. Process Biochem 34(5). doi: 10.1016/S0032-9592(98)00112-5.

Ho YSS, McKay G (1998) Sorption of Dye from Aqueous Solution by Peat. Chem Eng J 70(2):115–24. doi: https://doi.org/10.1016/S0923-0467(98)00076-1.

Ighnih H, Redouane H, Hassan O, Abdelmajid R, Brahim EI, Naima H, Amane J, Mohamed LT, Abdelaziz Ait A (2023) Efficient Removal of Hazardous Dye from Aqueous Solutions Using Magnetic Kaolinite Nanocomposite: Experimental and Monte Carlo Simulation Studies. Inorg Chem Commun 153. doi: 10.1016/j.inoche.2023.110886.

Issahaku I, Isaac KTe, Antonia YT (2023) Chitosan and Chitosan Derivatives: Recent Advancements in Production and Applications in Environmental Remediation. Environ Adv 11.

Kashi E, Surip SN, Tumirah K, Wan IN, Yannis DL, Zaher MY, Ali HJ (2024) High Adsorptive Performance of Chitosan-Microalgae-Carbon-Doped TiO2 (Kronos)/ Salicylaldehyde for Brilliant Green Dye Adsorption: Optimization and Mechanistic Approach. Int J Biol Macromol 259. doi: 10.1016/j.ijbiomac.2023.129147.

Kaur M, Monika D (2013) Adsorption Equilibrium and Kinetics of Toxic Dye-Erythrosine B Adsorption onto Montmorillonite. Sep Scı Technol 48(9). doi: 10.1080/01496395.2012.727939.

Kazemi J, Vahid J (2020) Alginate Beads Impregnated with Magnetic Chitosan@Zeolite Nanocomposite for Cationic Methylene Blue Dye Removal from Aqueous Solution. Int J Biol Macromol 154. doi: 10.1016/j.ijbiomac.2019.11.024.

Khan RI, Sarı A, Tuzen M, Lanjwani MF, Saleh TA (2023) Synthesis of Graphene/Silica Composites and Its Removal Efficiency of Methylene Blue Dye from Water. Inorg Chem Commun 158. doi: 10.1016/j.inoche.2023.111507.

Khapre MA, Sadanand P, Ravin MJ (2021) Glutaraldehyde-Cross-Linked Chitosan–Alginate Composite for Organic Dyes Removal from Aqueous Solutions. Int J Biol Macromol 190. doi: 10.1016/j.ijbiomac.2021.09.026.

Lai H, Gongke L, Zhuomin Z (2021) Ti3C2Tx-AgNPs@beta-Cyclodextrin SERS Substrate for Rapid and Selective Determination of Erythrosin B in Dyed Food. Sens Actuators B: Chem 346. doi: 10.1016/j.snb.2021.130595.

Langmuir I (1918) Adsorption of Gases on Glass, Mica and Platinum. J Am Chem Soc 40(1914):1361–1403.

Lima EC, Ahmad HB, Juan Carlos Moreno-Piraján, and Ioannis Anastopoulos. 2019. "A Critical Review of the Estimation of the Thermodynamic Parameters on Adsorption Equilibria. Wrong Use of Equilibrium Constant in the Van't Hoof Equation for Calculation of Thermodynamic Parameters of Adsorption." J Mol Liq 273. doi: 10.1016/j.molliq.2018.10.048.

Meng W, Hongnan S, Taihua M, Marco GV (2023) Pickering Emulsions with Chitosan and Macroalgal Polyphenols Stabilized by Layer-by-Layer Electrostatic Deposition. Carbohydr Polym 300:120256. doi: 10.1016/J.CARBPOL.2022.120256.

Mittal A, Jyoti M, Lisha K, Singh AK (2006) Process Development for the Removal and Recovery of Hazardous Dye Erythrosine from Wastewater by Waste Materials-Bottom Ash and De-Oiled Soya as Adsorbents. J Hazard Mater 138(1). doi: 10.1016/j.jhazmat.2006.05.038.

Nandanwar P, Ravin J, Vaishnavi G, Anita S, Apurva B, Dhandayutham S, Sadanand P (2023) Chitosan-Biopolymer-Entrapped Activated Charcoal for Adsorption of Reactive Orange Dye from Aqueous Phase and CO2 from Gaseous Phase. J Compos Sci 7(3). doi: 10.3390/jcs7030103.

Nannu S, Sripriya DRD, Dinesh KC, Gopikrishna M, Bhuvaneswari S, Udaya PNK (2023) Adsorption Kinetics, Equilibrium and Thermodynamics of a Textile Dye V5BN by a Natural Nanocomplex Material: Clinoptilolite. Energy Nexus 10. doi: 10.1016/j.nexus.2023.100197.

Nascimento RS, Corrêa JAM, Figueira BAM, Pinheiro PA, Silva JH, Freire PTC, Quaranta S (2022) From Mining Waste to Environmental Remediation: A Nanoadsorbent from Amazon Bauxite Tailings for the Removal of Erythrosine B Dye. Appl Clay Sci 222. doi: 10.1016/j.clay.2022.106482.

Pan X, Daoyong Z (2009) Removal of Malachite Green from Water by Firmiana Simplex Wood Fiber. Electron J Biotechnol 12(4). doi: 10.2225/vol12-issue4-fulltext-4.

Pipíška Ma, Eva KK, Milan H, Vladimír F, Libor Ď, Ivona Č, Mária K, Pellegrino C, and Gerhard S (2022) Biochar from Wood Chips and Corn Cobs for Adsorption of Thioflavin T and Erythrosine B. *Materials* 15(4). doi: 10.3390/ma15041492.

Raji Y, Ayoub N, Issam Me, Meriem S, Omar C, Souad Z (20239 High Adsorption Capacities of Crystal Violet Dye by Low-Cost Activated Carbon Prepared from Moroccan Moringa Oleifera Wastes: Characterization, Adsorption and Mechanism Study. Diam Relat Mater 135. doi: 10.1016/j.diamond.2023.109834.

Ramalakshmi RD, Murugan M, Jeyabal V (2022) Removal of Erythrosine B Using Prosopisspicigera L. Wood Carbon-Iron

Oxide Composite. Indian J Chem Technol 29(3). doi: 10.56042/ijct.v29i3.53865.

Rehan AI, Adiba IR, Awual ME, Waliullah RM, Mohammed SH, Khadiza TK, Md Shad S, Md Munjur H, Md Nazmul H, Md Chanmiya S, Hadi MM, Md Abdul K, Aminul I, Md Rabiul A (2023) Improving Toxic Dye Removal and Remediation Using Novel Nanocomposite Fibrous Adsorbent. Colloids Surf. A: Physicochem. Eng 673. doi: 10.1016/j.colsurfa.2023.131859.

Rytwo G, Huterer-Harari R, Dultz S, Gonen Y (2006) Adsorption of Fast Green and Erythrosin-B to Montmorillonite Modified with Crystal Violet. J Therm Anal Calorim 84(1). doi: 10.1007/s10973-005-7187-5.

Sabbagh N, Kambiz T, Amir AMS (2021) Application of Chitosan-Alginate Bio Composite for Adsorption of Malathion from Wastewater: Characterization and Response Surface Methodology. J Contam Hydro*l* 242. doi: 10.1016/j.jconhyd.2021.103868.

Sachan NK (2009) Sodium Alginate : The Wonder Polymer for Controlled Drug Delivery. J Pharm Res 2(7).

Sağlam S, Türk FN, Arslanoğlu H (2023) Use and Applications of Metal-Organic Frameworks (MOF) in Dye Adsorption: Review. J Environ Chem Eng 11(5).

Şen, Neşet Erek, and Zeynep Mine Şenol. 2023b. Effective Removal of Allura Red Food Dye from Water Using Cross-Linked Chitosan-Diatomite Composite Beads. Int J Biol Macromol 253:126632. doi: 10.1016/j.ijbiomac.2023.126632.

Şenol ZM (2021) A Chitosan-Based Composite for Adsorption of Uranyl Ions; Mechanism, Isothems, Kinetics and Thermodynamics. Int J Biol Macromol 183:1640–48. doi: 10.1016/j.ijbiomac.2021.05.130.

Şenol ZM, Elma E, El Messaoudi N, Mehmeti V (2023) Performance of Cross-Linked Chitosan-Zeolite Composite Adsorbent for Removal of Pb2+ Ions from Aqueous Solutions: Experimental and Monte Carlo Simulations Studies. J Mol Liq 391(July). doi: 10.1016/j.molliq.2023.123310.

Şenol ZM, Keskin ZS, Dinçer E, Ben Ayed Amina (2024) Influential Lead Uptake Using Dried and Inactivated-Fungal Biomass Obtained from Panaeolus Papilionaceus: Biological Activity, Equilibrium, and Mechanism. Biomass Convers Biorefin doi: 10.1007/s13399-024-05584-4.

Şenol ZM, El Messaoudi N, Fernine Y, Keskin ZS (2023) Bioremoval of Rhodamine B Dye from Aqueous Solution by Using Agricultural Solid Waste (Almond Shell): Experimental and DFT Modeling Studies. *Biomass Convers Biorefin* doi: 10.1007/s13399-023-03781-1.

Şenol ZM, Şimşek S (2020) Equilibrium, Kinetics and Thermodynamics of Pb(II) Ions from Aqueous Solution by Adsorption onto Chitosan-Dolomite Composite Beads. Int. J. Environ. Anal doi: 10.1080/03067319.2020.1790546.

Sharma P, Harleen K (2011) Sugarcane Bagasse for the Removal of Erythrosin B and Methylene Blue from Aqueous Waste. Appl Water Sci 1(3–4):135–45. doi: 10.1007/s13201-011-0018-x.

Tran ML, Tran TTV, Juang RS, Nguyen CH (2023) Graphene Oxide Crosslinked Chitosan Composites for Enhanced Adsorption of Cationic Dye from Aqueous Solutions. J Taiwan Inst Chem 142:104678. doi: 10.1016/j.jtice.2023.104678.

Umesh AS, Yashoda MP, Swathi T (2024) Enhanced Adsorption: Reviewing the Potential of Reinforcing Polymers and Hydrogels with Nanomaterials for Methylene Blue Dye Removal. J Surf Interfac Mater 51:104670. doi: 10.1016/j.surfin.2024.104670.

Wen Z, Ruihan P, Die G, Jing L, Jia Z, Zhou L, Famin K, Zhining X, Dandan W (2024) Chitosan-Alginate Sponge with Multiple Cross-Linking Networks for Adsorption of Anionic Dyes: Preparation, Property Evaluation, Mechanism Exploration, and Application. J Chromatogr A 1713. doi: 10.1016/j.chroma.2023.464507.

Wu FC, Ru LT, Ruey SJ (2009) Initial Behavior of Intraparticle Diffusion Model Used in the Description of Adsorption Kinetics. Chem Eng J 153(1–3). doi: 10.1016/j.cej.2009.04.042.

Zhang Z, Yu CH, Youyan L (2023) Efficient Antibacterial and Dye Adsorption by Novel Fish Scale Silver Biochar Composite Gel. Int J Biol Macromol 248. doi: 10.1016/j.ijbiomac.2023.125804.